






## Discoidin Domain Receptor-Driven Gene Signatures as Markers of Patient Response to Anti-PD-L1 Immune Checkpoint Therapy

Sungyong You, PhD <sup>1,2</sup> Minhyung Kim, PhD,<sup>1</sup> Xen Ping Hoi, PhD <sup>2,3</sup> Yu Cheng Lee, PhD,<sup>4</sup> Li Wang, PhD,<sup>5</sup> David Spetzler, PhD,<sup>6</sup> Jim Abraham, PhD <sup>6</sup> Dan Magee, PhD,<sup>6</sup> Prerna Jain, PhD <sup>7</sup> Matthew D. Galsky, MD,<sup>5</sup> Keith Syson Chan, PhD,<sup>2,3</sup> Dan Theodorescu, MD, PhD <sup>1,2,3,\*</sup>

<sup>1</sup>Department of Surgery, Cedars-Sinai Medical Center, Los Angeles, CA, USA; <sup>2</sup>Samuel Oschin Comprehensive Cancer Institute, Los Angeles, CA, USA; <sup>3</sup>Department of Pathology and Laboratory Medicine, Cedars-Sinai Medical Center, Los Angeles, CA, USA; <sup>4</sup>Graduate Institute of Medical Sciences, Taipei Medical University, Taipei, Taiwan; <sup>5</sup>Department of Medicine, Division of Hematology Oncology, Icahn School of Medicine at Mount Sinai, Tisch Cancer Institute, New York, NY, USA; <sup>6</sup>Caris Life Sciences, Irving, TX, USA; and <sup>7</sup>Tempus, Chicago, IL, USA

\*Correspondence to: Dan Theodorescu, MD, PhD, Samuel Oschin Comprehensive Cancer Institute, Cedars-Sinai Medical Center, 8700 Beverly Blvd, Los Angeles, CA 90048, USA (e-mail: Dan.Theodorescu@cshs.org).

### Abstract

**Background:** Anti-programmed cell death 1 (anti-PD-1) and PD ligand 1 (PD-L1) immune checkpoint therapies (ICTs) provided durable responses only in a subset of cancer patients. Thus, biomarkers are needed to predict nonresponders and offer them alternative treatments. We recently implicated discoidin domain receptor tyrosine kinase 2 (*DDR2*) as a contributor to anti-PD-1 resistance in animal models; therefore, we sought to investigate whether this gene family may provide ICT response prediction. **Methods:** We assessed mRNA expression of *DDR2* and its family member *DDR1*. Transcriptome analysis of bladder cancer (BCa) models in which *DDR1* and 2 were perturbed was used to derive *DDR1*- and *DDR2*-driven signature scores. *DDR* mRNA expression and gene signature scores were evaluated using BCa–The Cancer Genome Atlas ( $n = 259$ ) and IMvigor210 ( $n = 298$ ) datasets, and their relationship to BCa subtypes, pathway enrichment, and immune deconvolution analyses was performed. The potential of *DDR*-driven signatures to predict ICT response was evaluated and independently validated through a statistical framework in bladder and lung cancer cohorts. All statistical tests were 2-sided. **Results:** *DDR1* and *DDR2* showed mutually exclusive gene expression patterns in human tumors. *DDR2*<sup>high</sup> BCa exhibited activation of immune pathways and a high immune score, indicative of a T-cell-inflamed phenotype, whereas *DDR1*<sup>high</sup> BCa exhibited a non-T-cell-inflamed phenotype. In IMvigor210 cohort, tumors with high *DDR1* (hazard ratio [HR] = 1.53, 95% confidence interval [CI] = 1.16 to 2.06;  $P = .003$ ) or *DDR2* (HR = 1.42, 95% CI = 1.01 to 1.92;  $P = .04$ ) scores had poor overall survival. Of note, *DDR2*<sup>high</sup> tumors from IMvigor210 and CheckMate 275 ( $n = 73$ ) cohorts exhibited poorer overall survival (HR = 1.56, 95% CI = 1.20 to 2.06;  $P < .001$ ) and progression-free survival (HR = 1.77, 95% CI = 1.05 to 3.00;  $P = .047$ ), respectively. This result was validated in independent cancer datasets. **Conclusions:** These findings implicate *DDR1* and *DDR2* driven signature scores in predicting ICT response.

Immune checkpoint therapies (ICTs) are emerging as an important pillar of anticancer therapy (1–3). ICTs target co-inhibitory receptors on T cells, such as programmed cell death 1 (PD-1), PD-1 ligand 1 (PD-L1), and cytotoxic T lymphocyte-associated protein 4 (4). Despite many durable clinical responses in melanoma, non-small cell lung carcinoma (NSCLC), bladder cancer (BCa), and renal cell cancer (4), many patients are nonresponders (5,6). In an attempt to stratify response, biomarkers including PD-L1 overexpression on cancer cells or immune cells, tumor mutational burden (TMB), microsatellite instability, and neoantigen load have been studied (4). Although there are

associations between these biomarkers and ICT outcomes, neither PD-L1 overexpression nor TMB as a single marker can distinguish ICT responders from nonresponders (7,8). A meta-analysis of 45 studies using ICTs showed that PD-L1 overexpression in cancer or immune cells was predictive in only 28.9% cases and not predictive or not tested in the remaining 53.3% and 17.8% cases, respectively (9). These studies highlight the need to improve or identify new biomarkers for stratifying ICT responses, which is the objective of the current study.

We recently identified discoidin domain receptor 2 (*DDR2*) expression as a determinant of ICT response in murine models

Received: June 4, 2021; Revised: December 10, 2021; Accepted: July 14, 2022

© The Author(s) 2022. Published by Oxford University Press. All rights reserved. For permissions, please email: journals.permissions@oup.com

of BCa and then used genetic and pharmacologic methods to show that *DDR2* inhibition can sensitize murine BCa ICT response (10). Interestingly, *DDR2* inhibition alone did not influence murine BCa growth. Therefore, we reasoned that signatures composed of genes modulated by *DDR2*, or its family member *DDR1*, can possibly stratify patient response to ICT. Here, we show that scores generated from such gene signatures can stratify response to anti-PD-L1 therapy in BCa and NSCLC.

## Methods

### Institutional Review Board Approval

All human data were obtained from previously reported sources and references in publications.

### Statistical Analysis

We performed a secondary analysis of existing published transcriptome datasets from The Cancer Genome Atlas (TCGA) and IMvigor210 studies, which are publicly available. Signature score computation using deidentified transcriptome data to validate the signature performance without direct access to identifiable patient clinical data on 2 NSCLC datasets (from authors from Caris and Tempus) and CheckMate 275 dataset (from authors from Icahn School of Medicine) was performed. A  $\chi^2$  test was used to test inverse relationship of *DDR1* and *DDR2* (*DDR1/2*) gene expression in BCa. Association of clinical outcomes was assessed using Kaplan-Meier survival curves and log-rank and/or Cox statistics. To test whether *DDR* signature performance was prognostic independent of other clinical variables, multi-variable analyses were performed adjusting for the age, sex, grade, and stage when it is available. A *P* value less than .05 was considered statistically significant. We used the MATLAB package including the Statistics toolbox (Mathworks, Natick, MA, USA), the R package (v.4.1 <http://www.r-project.org/>) for all statistical tests, and computational analysis.

## Results

### Gene Expression of *DDR1/2* in BCa

We have reported the roles of the *DDR* family, *DDR1/2*, in modulating BCa metastasis and ICT response (10,11). Unsupervised clustering of *DDR1/2* expression from the TCGA-BCa cohort (*n* = 259) (Table 1) (12) suggested that tumors could be divided into *DDR1*<sup>high</sup>*DDR2*<sup>low</sup> and *DDR1*<sup>low</sup>*DDR2*<sup>high</sup> groups (Figure 1, A;  $\chi^2$  *P* < .001), with *DDR1/2* expression exhibiting an inverse relationship (Figure 1, B; Spearman  $\rho$  = -0.27).

Because gene expression-based BCa subtypes associate with different clinical behaviors (12,13), we investigated the distribution of high *DDR1* and *DDR2* tumors among luminal papillary (LumP), basal and squamous (Ba/Sq), luminal unstable, stromal-rich, luminal nonspecified, and neuroendocrine-like subtypes (Figure 1, C). The LumP subtype has a high proportion of *DDR1*<sup>high</sup> tumors and overall *DDR1* expression (Figure 1, C, D;  $\chi^2$  *P* = .002), whereas the stroma-rich subtype has a higher proportion of *DDR2*<sup>high</sup> tumors (Figure 1, C, E). The stark difference between these 2 subtypes is intriguing and may reflect the expression of *DDR2* in both cancer cells and stromal fibroblasts in the tumor microenvironment (TME) (14).

**Table 1.** Clinicopathological characteristics of TCGA BCa cohort by *DDR* expression levels (*n* = 259<sup>a</sup>)

Characteristics	Level of <i>DDR1</i> and <i>DDR2</i> gene expression			
	<i>DDR1</i> <sup>high</sup> and <i>DDR2</i> <sup>high</sup>	<i>DDR1</i> <sup>high</sup> and <i>DDR2</i> <sup>low</sup>	<i>DDR1</i> <sup>low</sup> and <i>DDR2</i> <sup>high</sup>	<i>DDR1</i> <sup>low</sup> and <i>DDR2</i> <sup>low</sup>
Sex				
Female	10	22	26	12
Male	39	58	54	38
Pathologic stage				
II	10	34	12	12
III	17	27	37	24
IV	22	19	31	14
T stage				
T2	11	39	13	14
T3	28	33	54	28
T4	10	8	13	8
Recurrent				
No	17	40	28	18
Recurrent	2	10	5	5
Not specified	30	30	47	27
Overall survival				
Living	24	53	40	29
Deceased	25	27	40	29
Histological grade				
High grade	49	80	80	50
Low grade	0	0	0	0

<sup>a</sup>From a total of 407 samples, 259 samples were selected by filtering with the following criteria: 1) any stage other than T2-T4; 2) 52 (13%) had urothelial carcinoma with variant histology, including 42 squamous, 4 small cell and/or neuroendocrine, 2 micropapillary, and 4 plasmacytoid; 3) 5 additional tumors that met screening criteria were included: 3 pure squamous cell bladder carcinomas, 1 squamous cell carcinoma of nonbladder origin and 1 bladder adenocarcinoma; 4) from a total of 57 patients, 35 had received prior intravesical immunotherapy with Bacille Calmette-Guerin; 5) 12 patients had received neoadjuvant chemotherapy. BCa = bladder cancer; *DDR* = discoidin domain receptor; TCGA = The Cancer Genome Atlas.

These findings suggest that the classical BCa subtypes are more heterogeneous than previously thought, and their clinical behavior may in part be driven by *DDR1/2* expression. Given this, we examined if *DDR1/2* expression stratified patient outcomes in TCGA-BCa. *DDR1*<sup>high</sup> tumors trended toward a better overall survival (OS), but this was not statistically significant (hazard ratio [HR] = 0.96, 95% confidence interval [CI] = 0.74 to 1.46; *P* = .73), whereas *DDR2*<sup>high</sup> tumors had statistically significantly poorer OS (HR = 1.55, 95% CI = 1.04 to 2.26; *P* = .02; Figure 1, F).

### The Bladder Tumor Microenvironment in *DDR1*<sup>high</sup> and *DDR2*<sup>high</sup> Tumors

Gene set enrichment analysis (GSEA) identified 16 statistically significantly enriched cellular processes in *DDR2*<sup>high</sup> compared with *DDR2*<sup>low</sup> tumors, which were not enriched in *DDR1*<sup>high</sup> tumors (Figure 2, A). Epithelial mesenchymal transition (EMT) and Extracellular matrix (ECM) receptor interaction were statistically significantly enriched in *DDR2*<sup>high</sup> tumors (Figure 2, A), echoing the higher prevalence of *DDR2*<sup>high</sup> tumors in the stroma-rich subtype (Figure 1, C). Intriguingly, transforming growth factor- $\beta$  signaling pathway and wingless/integrated (WNT) signaling pathway were enriched in both *DDR1*<sup>high</sup> and

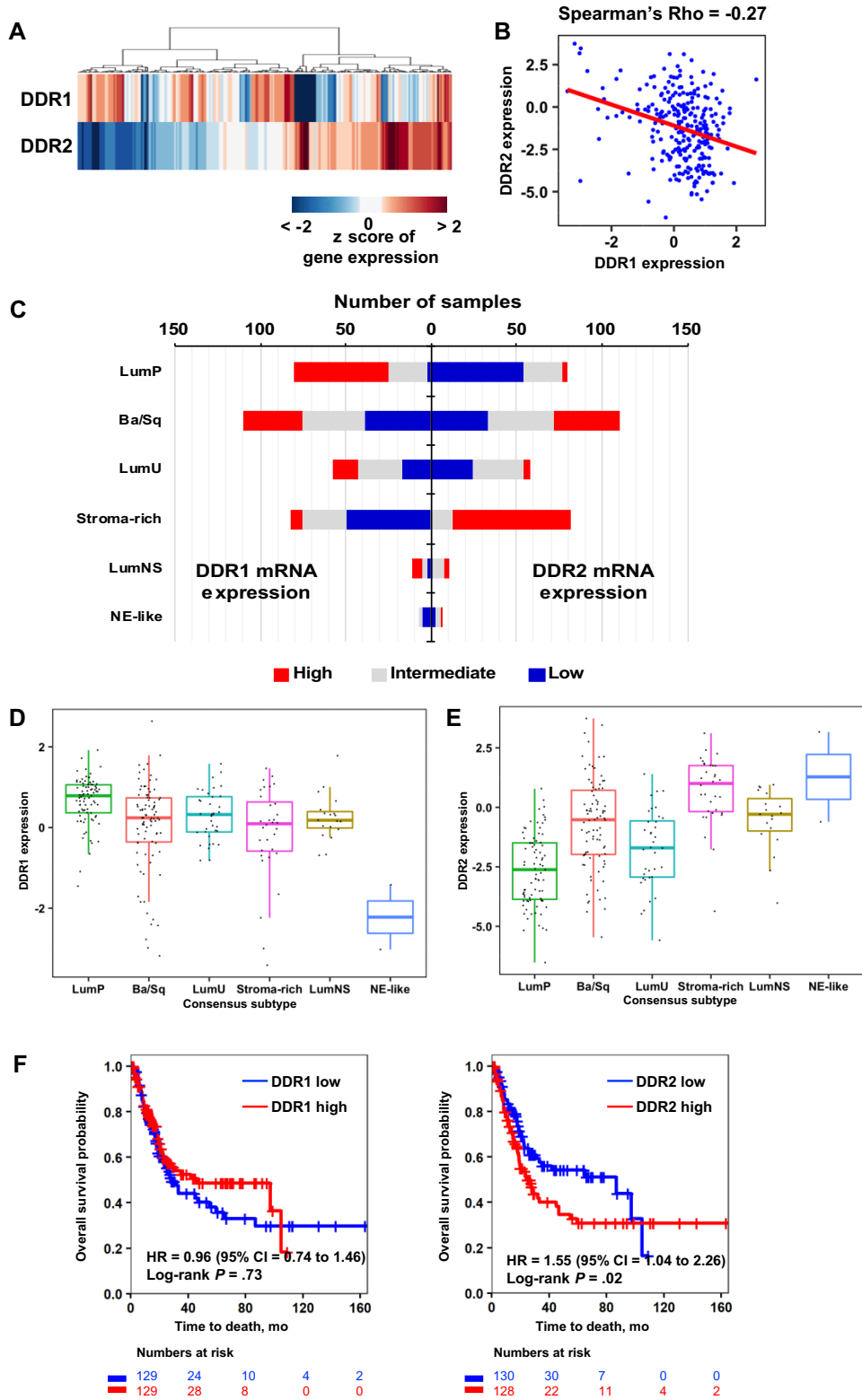


**Figure 1.** Expression of DDR genes in human bladder tumors as a function of molecular subtype and clinical outcome. **A)** Heatmap depicts expression pattern of DDR1 and DDR2 in the TCGA-BCa cohort described in “Materials” and “Methods” (n = 259). **B)** Scatter plot and regression line (red) shows an inverse relationship between DDR1 and DDR2 expression. Hierarchical clustering was performed using the Manhattan distance and ward linkage method. **C)** Stacked bar graphs depict the distribution of tumors from the TCGA-BCa cohort by bladder cancer consensus subtypes (13). Tumor samples in each subtype were stratified into 3 groups by DDR expression at tertile values. **D and E)** Box plots show DDR1 (**D**) and DDR2 (**E**) expression in BCa consensus subtypes. **F)** Kaplan-Meier survival curves for DDR1 and DDR2 expression in the TCGA BCa cohort. Tumors were stratified into high and low groups at median expression of DDR. Statistical significance of differential survival between the groups were tested by log-rank test. Ba/Sq = basal and squamous; BCa = bladder cancer; CI = confidence interval; DDR = discoidin domain receptor; HR = hazard ratio; LumNS = luminal nonspecified; LumP = luminal papillary; LumU = luminal unstable; NE = neuroendocrine; TCGA = The Cancer Genome Atlas.

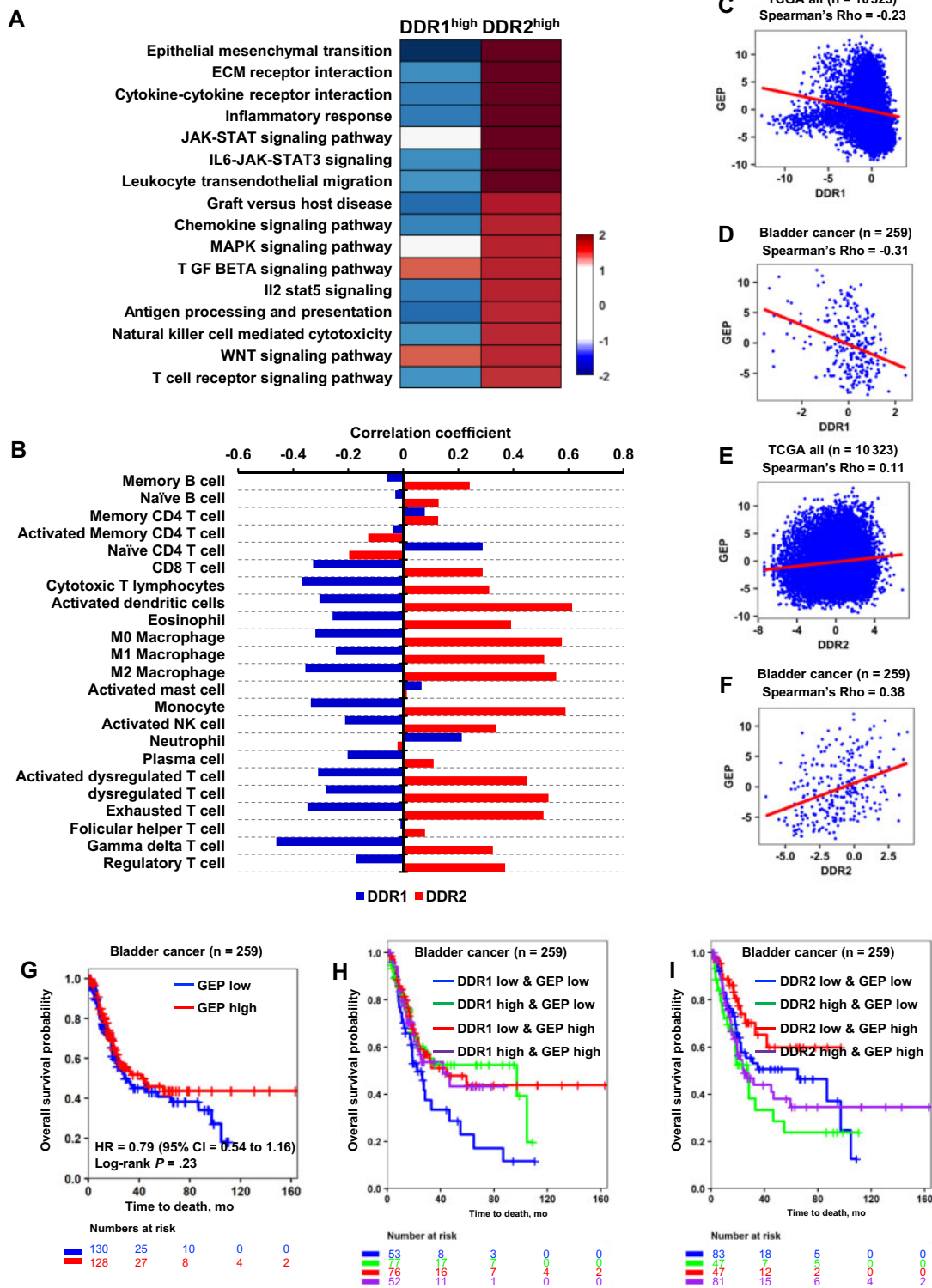


**Figure 2.** Impact of DDR expression on gene set enrichment analysis, molecularly defined cellular composition, and T-cell-inflamed GEP in human bladder tumors. **A)** Heatmap displays differentially enriched hallmark gene sets between DDR1<sup>high</sup> and DDR2<sup>high</sup> bladder tumors. Color bar represents the log-two-fold change of the DDR1 or DDR2 high group compared with the DDR1 or DDR2 low group. **B)** Bar graphs depict Spearman correlation coefficient of DDR1/2 expression and 23 immune infiltration scores described in "Materials" and "Methods." **C-F)** TCGA pan-cancer patients (n = 10,323) and TCGA-BCa patients (n = 259) analysis of DDR1/2 expression and T-cell-inflamed GEP score shows negative correlation with DDR1 expression (**C, D**) and positive correlation with DDR2 expression (**E, F**). Spearman method was used to estimate the correlation coefficient. The red line indicates the regression line. **G)** Tumors were stratified by T-cell-inflamed GEP score at the median of the TCGA-BCa patients (n = 259). **H)** Survival curves shows survival patterns of the 4 groups by DDR1 expression and T-cell-inflamed GEP score. Multiple log-rank tests were performed with the DDR1<sup>low</sup> and GEP<sup>low</sup> group as a base line. **I)** Survival curves show survival patterns of the 4 groups by DDR2 and T-cell-inflamed GEP score. BCa = bladder cancer; CI = confidence interval; DDR = discoidin domain receptor; GEP = gene-expression profile; HR = hazard ratio; TCGA = The Cancer Genome Atlas; ECM = extracellular matrix; JAK = Janus kinase; STAT = signal transducer and activator of transcription; IL6 = interleukin 6; NK = natural killer; MAPK = mitogen-activated protein kinase; TGF = transforming growth factor; IL2 = interleukin 2; WNT = wingless/integrated.

DDR2<sup>high</sup> tumors (Figure 2, A). Another key finding is the enrichment of immune cell-related processes, such as cytokine-cytokine receptor interaction, inflammatory response, and T-cell receptor signaling in DDR2<sup>high</sup> tumors (Figure 2, A), indicative of a DDR2 role in immune regulation and suggesting a T-cell-inflamed phenotype that is ineffectual in immune rejection of the tumors (15). In contrast, DDR1<sup>high</sup> tumors have statistically significant enrichment in P53 pathway (Normalized Enrichment Score [NES] = 1.51;  $P = .003$ ), estrogen response early (NES = 1.48;  $P = .002$ ), and protein secretion (NES = 1.45;  $P = .009$ ). This suggests that DDR1<sup>high</sup> tumors are positive in distinct cellular functions from DDR2<sup>high</sup> tumors and negatively associated with these immune cell-related processes (Figure 2, A), proposing that they are non-T-cell inflamed.

Next, we assessed the correlation between DDR1/2 expression levels and 23 immune cell signatures (Supplementary Table 1, available online). Consistent with the GSEA results (Figure 2, A), the correlation coefficients of immune cell types demonstrated reciprocal values between DDR1<sup>high</sup> and DDR2<sup>high</sup> tumors in TCGA-BCa (Figure 2, B). DDR2<sup>high</sup> tumors were positively correlated with 19 immune cells (Figure 2, B), indicative of an immunologically “hot” TME. Conversely, DDR1<sup>high</sup> tumors were negatively correlated with most immune cells (Figure 2, B), indicative of an immunologically “cold” TME. These indicate that distinct TMEs are present in DDR1<sup>high</sup> and DDR2<sup>high</sup> BCa, suggesting these 2 genes have differential biological roles despite their structural similarity (16-18).

We also found that DDR1 expression was inversely correlated with the T-cell-inflamed gene-expression profile (GEP) score in both the TCGA-pan-cancer cohort ( $n = 10\,323$ ) (Figure 2, C;  $\rho = -0.23$ ,  $P < .001$ ) and TCGA-BCa (Figure 2, D;  $\rho = -0.31$ ,  $P < .001$ ), whereas DDR2 expression was positively correlated (Figure 2, E;  $\rho = 0.11$ ,  $P < .001$ ; Figure 2, F;  $\rho = 0.38$ ,  $P < .001$ ). DDR2 expression was also statistically significantly correlated with the presence of CD8+ T cells ( $\rho = 0.29$ ,  $P < .001$ ) and cytotoxic T lymphocytes ( $\rho = 0.31$ ,  $P < .001$ ) in the TCGA-BCa (Figure 2, B).

Because GEP score is known to be associated with ICT responsiveness, we tested whether DDR expression in addition to GEP score has an additional benefit in identifying patients with distinct survival. GEP score alone had no statistically significant association with OS in TCGA-BCa (Figure 2, G). However, GEP scores stratified by DDR1/2 expression exhibited differences. The DDR1<sup>low</sup>GEP<sup>low</sup> group showed worse OS compared with the DDR1<sup>high</sup>GEP<sup>low</sup> and DDR1<sup>low</sup>GEP<sup>high</sup> groups (Figure 2, H, Table 2). Additionally, the DDR2<sup>low</sup> groups (ie, DDR2<sup>low</sup>GEP<sup>low</sup>, DDR2<sup>low</sup>GEP<sup>high</sup>) exhibited better OS compared with DDR2<sup>high</sup> groups (ie, DDR2<sup>high</sup> and GEP<sup>low</sup> and DDR2<sup>high</sup> and GEP<sup>high</sup>) (Figure 2, I; Table 2). This indicates that DDR expression offers better predictive information compared with GEP scores.

### Association of DDR Expression and Response to ICT

DDR1<sup>high</sup> and DDR2<sup>high</sup> tumors appear to associate with immunologically cold and hot TMEs, respectively, whereas DDR2<sup>high</sup> tumors have worse patient outcome following surgery. Given these associations, we investigated the relationship of DDR1/2 expression in patients undergoing ICT (19). Using the IMvigor210 dataset, where BCa patients were treated with atezolizumab anti-PD-L1<sup>19</sup>, we assessed if DDR1/2 expression associates with immune infiltration. Consistent with the TCGA-BCa results, IMvigor210 showed similar patterns of correlation between DDR1/2 expression and immune infiltration scores of immune cells (Figure 3, A). Unsupervised clustering analysis of

**Table 2.** Multiple log-rank tests were performed with DDR1<sup>low</sup> and GEP<sup>high</sup> group as baseline in TCGA BCa and IMvigor<sup>a</sup>

Comparison	HR (95% CI)	P	Cohort
DDR1 <sup>high</sup> and GEP <sup>low</sup> vs DDR1 <sup>low</sup> and GEP <sup>low</sup>	0.65 (0.39 to 1.10)	.11	TCGA BCa
DDR1 <sup>low</sup> and GEP <sup>high</sup> vs DDR1 <sup>low</sup> and GEP <sup>low</sup>	0.58 (0.35 to 0.97)	.04	TCGA BCa
DDR1 <sup>high</sup> and GEP <sup>high</sup> vs DDR1 <sup>low</sup> and GEP <sup>low</sup>	0.73 (0.42 to 1.27)	.26	TCGA BCa
DDR2 <sup>low</sup> and GEP <sup>low</sup> vs DDR2 <sup>low</sup> and GEP <sup>high</sup>	1.86 (0.98 to 3.53)	.06	TCGA BCa
DDR2 <sup>high</sup> and GEP <sup>low</sup> vs DDR2 <sup>low</sup> and GEP <sup>high</sup>	2.61 (1.33 to 5.12)	.005	TCGA BCa
DDR2 <sup>high</sup> and GEP <sup>high</sup> vs DDR2 <sup>low</sup> and GEP <sup>high</sup>	2.19 (1.16 to 4.13)	.02	TCGA BCa
DDR1 <sup>high</sup> and GEP <sup>low</sup> vs DDR1 <sup>low</sup> and GEP <sup>low</sup>	0.79 (0.55 to 1.14)	.20	IMvigor
DDR1 <sup>low</sup> and GEP <sup>high</sup> vs DDR1 <sup>low</sup> and GEP <sup>low</sup>	0.76 (0.53 to 1.10)	.15	IMvigor
DDR1 <sup>high</sup> and GEP <sup>high</sup> vs DDR1 <sup>low</sup> and GEP <sup>low</sup>	1.13 (0.80 to 1.60)	.48	IMvigor
DDR2 <sup>low</sup> and GEP <sup>low</sup> vs DDR2 <sup>low</sup> and GEP <sup>high</sup>	0.76 (0.53 to 1.12)	.17	IMvigor
DDR2 <sup>high</sup> and GEP <sup>low</sup> vs DDR2 <sup>low</sup> and GEP <sup>high</sup>	1.05 (0.74 to 1.51)	.78	IMvigor
DDR2 <sup>high</sup> and GEP <sup>high</sup> vs DDR2 <sup>low</sup> and GEP <sup>high</sup>	0.89 (0.62 to 1.29)	.53	IMvigor

<sup>a</sup>BCa = bladder cancer; CI = confidence interval; DDR = discoidin domain receptor; GEP = gene-expression profile; HR = hazard ratio; TCGA = The Cancer Genome Atlas.

DDR1/2 expression showed separation of DDR1<sup>high</sup>DDR2<sup>low</sup> vs DDR1<sup>low</sup>DDR2<sup>high</sup> tumors with an inverse linear relationship ( $\rho = -0.45$ ,  $P < .001$ ) (Figure 3, B). DDR1/2 expression had no correlation with ICT response (Figure 3, C-F) or patient survival (Figure 3, G, H), even when DDR expression was further stratified by GEP scores (Figure 3, I and J; Table 2).

### Development of DDR-Driven Gene Signatures

The lack of outcome stratification by DDR1/2 expression led us to explore a broader evaluation of DDR-regulated gene expression. We hypothesized expression changes would represent biologically active DDR signaling rather than just high DDR expression with minimal downstream transcriptional consequences. We developed gene signatures that were sensitive to changes in DDR1/2 expression (20). We either overexpressed DDR1 (DDR1-OE) or depleted DDR2 (DDR2-KD) in BCa models. Subcutaneous tumors in mice generated from either DDR1-OE T24 human BCa cells and controls. In these experiments, female Rag2 and Il2rg double-knockout mice (Taconic) were used. Four mice per group were used with tumors removed 6 weeks after initial tumor cell inoculation and profiled. The details of the DDR2 experiments were described in our prior publication (10,21) and carried out on tumors derived from a murine cell line NA13 BCa (10,21) transduced with shDDR2 or scrambled shRNA, subjected to RNA-sequencing (Supplementary Figure 1, A, available online). Differential expression analysis was performed (Supplementary Figure 1, B, C, available online). A total of 225 upregulated and 367 downregulated genes (Supplementary Table 2, available online) by DDR1-OE, and 211 upregulated and 69 downregulated genes (Supplementary Table

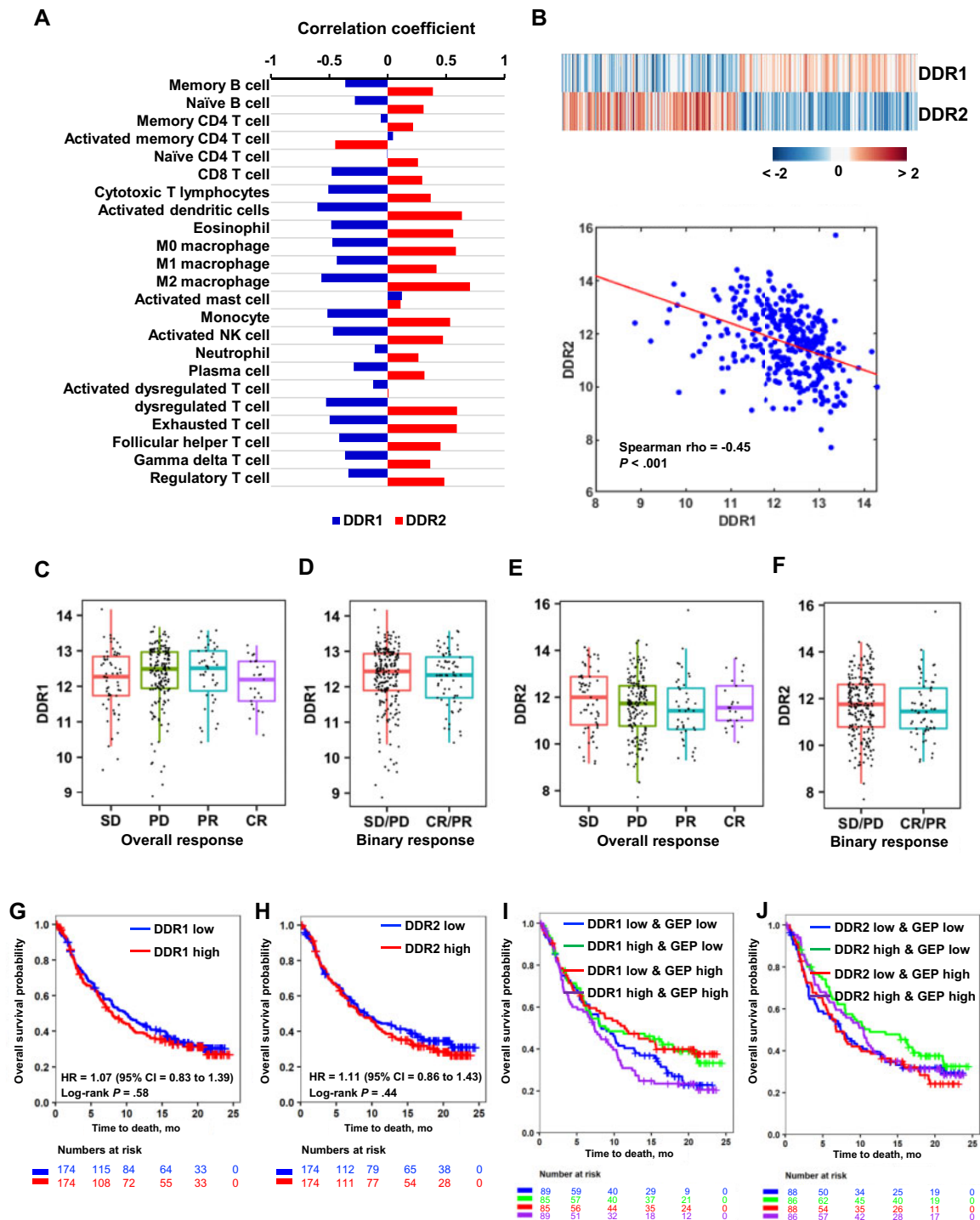


**Figure 3.** Association of DDR expression with TME features and immune checkpoint therapy response in human BCa. **A)** Bar graph depicts Spearman correlation coefficients of DDR1 and DDR2 expression with immune cell type scores ( $n = 23$ ). **B)** Heatmap and scatter plot show an inverse relationship of DDR1 and DDR2 expression in the IMvigor cohort. Color bar represents the z score of gene expression. **C, D)** Box plots depict expression distribution of DDR1 by immunotherapy response groups in the IMvigor210 cohort ( $n = 298$ ). **E, F)** Box plots depict expression distribution of DDR2 by immunotherapy response groups in IMvigor ( $n = 298$ ). **G, H)** Kaplan-Meier (KM) survival curves for DDR1 (**G**) and DDR2 (**H**) expression in IMvigor. Tumors were stratified into high and low groups at median expression of DDR. Significance of differential survival between the groups was tested by log-rank test. **I)** KM curves show survival patterns of the 4 groups by DDR1 expression and T-cell-inflamed GEP score. Multiple log-rank tests were performed with  $DDR1^{low}$  and  $GEP^{low}$  group as a baseline. **J)** KM curves show survival patterns of the 4 groups by DDR2 and T-cell-inflamed GEP score. Multiple log-rank tests were performed with  $DDR2^{low}$  and  $GEP^{high}$  group as a baseline. **Table 2** show hazard ratio, significance level ( $P$  value), and confidence interval for each comparison. BCa = bladder cancer; CI = confidence interval; CR = complete response; DDR = discoidin domain receptor; GEP = gene-expression profile; HR = hazard ratio; PD = partial disease; PR = partial response; SD = stable disease; TCGA = The Cancer Genome Atlas; TGF = transforming growth factor; TME = tumor microenvironment.

3, available online) by DDR2-KD were identified with a false discovery rate less than .05 and log<sub>2</sub>-fold-change of at least 1. Functional enrichment analysis using DAVID (22) of 225 upregulated genes by DDR1-OE and 69 downregulated genes by DDR2-KD revealed statistically significant and specific enrichment of epithelial development and excretion by DDR1-OE (Supplementary Figure 1, D, available online) and chemokine signaling and immune and/or inflammatory responses by DDR2-KD (Supplementary Figure 1, E, available online). Regulation of cell proliferation and wound response were similarly enriched by both DDR1 and DDR2 manipulations (Supplementary Figure 1, F, available online).

From the 225 upregulated genes by DDR1-OE and 69 downregulated genes by DDR2-KD (Supplementary Figure 2, A, available online), we first selected the top 50 most differentially expressed genes (Supplementary Figure 2, B, available online) because recent data from a large-scale transcriptome analysis revealed that the top 50 ranked genes usually provided markers that discriminate between experimental groups with high confidence (23,24). These 2 sets of genes had no overlap. We used them to compute DDR1/2 activity scores and examined their association with molecular functions, clinical, and therapeutic outcomes (Supplementary Figure 2, B, available online).

Next, we stratified IMvigor210 patients into DDR1/2-high and -low median score groups (25). GSEA were performed, and the top 10 KEGG pathways statistically significantly enriched in DDR1- or DDR2-high score tumors are presented in Figure 4, A and B. Consistent with the enriched gene sets in Figure 2, A, DDR2<sup>high</sup> tumors exhibited statistically significant enrichment of immune-related pathways (Figure 4, A), whereas DDR1<sup>high</sup> tumors enriched for metabolic pathways (Figure 4, B). LumP and Ba/Sq subtypes had the largest fractions of tumors with high DDR1/2 scores (Figure 4, C).

### Evaluation of DDR Signature Scores as Predictors of Anti-PD-L1 Response in Patients

Next, we examined the ability of the DDR signature scores to stratify ICT response and survival from IMvigor210. DDR scores were statistically significantly different between stable disease or partial disease and complete response or partial response ( $P < .001$  for DDR1 and  $P < .001$  for DDR2) (Figure 5, A and B). Furthermore, tumors with high DDR1 (HR = 1.51, 95% CI = 1.16 to 2.06;  $P = .003$ ) (Figure 5, C) or high DDR2 (HR = 1.42, 95% CI = 1.01 to 1.92;  $P = .04$ ) (Figure 5, D) scores had poorer OS, suggesting that DDR scores have the potential to discriminate between patients with differential responses to anti-PD-L1 therapy.

To optimize the composition of the DDR gene signature, we selected core genes among the 50 that were highly associated with OS in IMvigor210 through a statistical framework (Figure 6, A; see Supplementary Methods, available online), resulting in gene signatures for risk stratification of patients: a 10-gene signature based on a z score model (CS-10) and a 19-gene signature based on a Cox model (CS-19) for DDR1 and a 4-gene signature based on a z score model (CS-4) and a 25-gene signature based on a Cox model (CS-25) for DDR2.

We also surveyed optimal cut points of the signature score using IMvigor210 data by assessing hazard ratios across all DDR signature scores for OS. We identified optimal cut points of CS-10, CS-19, CS-4, and CS-25, which are -0.77, -0.079, 0.039, and -0.059, respectively. Survival differences at these cut points are all statistically significant (Figure 6, B, C). We also assessed survival association of the DDR signature scores in BCa consensus

subtypes. The LumP and Ba/Sq subtypes with high CS-10 (Figure 6, D) and CS-19 (Figure 6, E) scores were associated with worse OS, whereas the stroma-rich subtype with high CS-4 (Figure 6, F) or high CS-25 (Figure 6, G) scores were associated with worse OS. Of note, CS-25 showed the best performance in the stroma-rich subtype and statistically significant stratification of OS in all subtypes. We further made 2 combined models by union of CS-10 and CS-4 models for combined DDR z score model (CS-14) and union of CS-19 and CS-25 Cox models for combined DDR Cox model (CS-44). CS-14 and CS-44 gene models have better association with OS compared with DDR1 or DDR2 models before combining with a better hazard ratio of 2.03 (95% CI = 1.53 to 2.71;  $P < .001$ ) and 2.48 (95% CI = 1.85 to 3.33;  $P < .001$ ), respectively (Supplementary Figure 3, available online).

Next, we identified RNA-sequencing and outcome data from 2 NSCLC cohorts (ie, Tempus and Caris) treated with anti-PD-L1 in routine practice. We applied our scoring of the 4-gene signatures to these. This analysis was done in a double-blinded fashion. The survival curves were computed by investigators with the patient DDR signature scores but no information on gene composition or how the score was derived. Clinical characteristics are described in Supplementary Table 4 (available online). Notably, the 2 NSCLC cohorts had differences in the proportion of PD-L1-stained tumor-infiltrating lymphocyte (TIL) immune cells, with 29% of tumors ( $n = 59$ ) in the Tempus cohort having more than 5% of PD-L1-positive cells compared with 50% of tumors ( $n = 129$ ) in the Caris cohort. This may explain why CS-4 high and low groups exhibited statistically significant survival differences in the Tempus cohort (HR = 1.47, 95% CI = 1.03 to 2.10;  $P = .04$ ; Figure 6, H), whereas CS-25 high and low groups exhibited statistically significant survival differences in the Caris cohort (HR = 2.55, 95% CI = 1.28 to 5.09;  $P = .008$ ; Figure 6, I). Both CS-4 and CS-25 are DDR2 signature scores, and the survival difference with CS-4 shows a higher hazard ratio compared with CS-25 in the stroma-rich subtype (Figure 6, F and G). We also evaluate the performance of CS-4 with an independent cohort from CheckMate 275 study (26), a dataset comprised of patients with metastatic urothelial cancer treated with the PD-1 inhibitor nivolumab, and found statistically significant poorer survival in CS-4 high tumors (HR = 1.77, 95% CI = 1.05 to 3.00;  $P = .046$ ; Figure 6, J) consistent with the statistically significant difference of CS-4 scores between complete response or partial response and stable disease or partial disease groups ( $P = .02$ ; Figure 6, K). Along with this, we further assessed DDR2 signature scores in 6 independent cohorts (4 melanoma, 1 glioblastoma, and 1 with metastatic urothelial carcinoma) with checkpoint inhibitors responses (Supplementary Figure 4, available online).

### Discussion

Biomarkers for stratifying ICT responses can be broadly categorized into 2 subsets: biomarkers indicative of a T-cell-inflamed TME and genomic biomarkers. The expression of PD-L1 is associated with clinical response to ICT in multiple cancers including melanoma, NSCLC, renal cell carcinoma, and colon cancer (27-30). However, PD-L1 can be expressed on tumor and immune cells, and the predictive value of PD-L1 expression on either tumor or immune cells differs based on the cancer type (29,31-33). Additionally, challenges exist interpreting PD-L1 expression by immunohistochemistry, because of variability in antibodies and scoring methods (34). More important, some studies show that patients with PD-L1-negative tumors can also

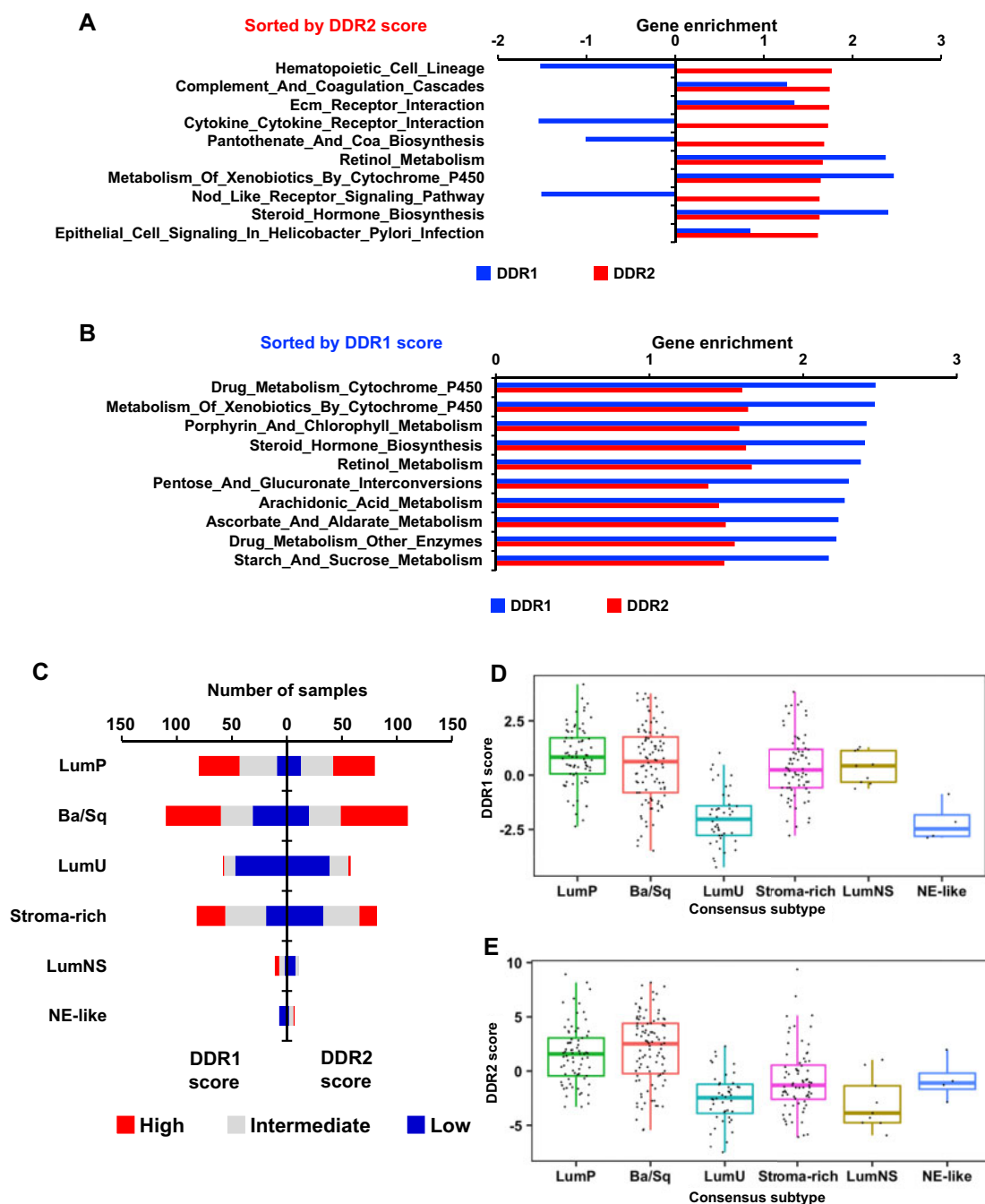


**Figure 4.** Relationship of DDR gene signature scores with molecular pathways and tumor subtypes in bladder cancer. **A, B** Bar plots depict enrichment of KEGG pathways by DDR2 (**A**) or DDR1 (**B**) active tumors. DDR1/2 gene expression score was computed by a z score method and used to stratify tumors into 2 groups with high and low DDR1 or DDR2 scores. Pathways were sorted by their DDR score, and the top 10 pathways were selected. **C**) Stacked bar graph depicts distribution of the tumors from IMvigor by BCa consensus subtypes. Tumor samples in each subtype were stratified into 3 groups by DDR score at tertile values. **D, E**) Box plot shows DDR1 (**D**) and DDR2 (**E**) scores in BCa consensus subtypes in IMvigor. Ba/Sq = basal and squamous; BCa = bladder cancer; DDR = discoidin domain receptor; LumNS = luminal nonspecified; LumU = luminal unstable; NE = neuroendocrine.

benefit from ICT (35,36), suggesting the presence of biological drivers of response unrelated to PD-L1.

Other parameters evaluated as predictors of ICT response include 1) the presence of TILs (29), 2) T-cell-inflamed GEP (37), and 3) interferon (IFN)- $\gamma$  gene signature (38). In general, high densities of TILs (ie, CD8<sup>+</sup> T cells) have been associated with better clinical outcome after surgical removal of primary tumors (39). In the context of ICT, targeting PD-1 and PD-L1 signaling is

thought to reinvigorate preexisting antitumor response of TILs, which express immune checkpoint molecules (40). IFN- $\gamma$  is a cytokine released by activated T cells, nature killer cells, and natural killer T cells and is important for both antitumor response and adaptive immune resistance mechanisms. IFN- $\gamma$  signaling also upregulates expression of PD-L1 on tumor, stromal, and other immune infiltrating cells, which can interact with PD-1 on TILs (41). Genomic biomarkers such as TMB and microsatellite



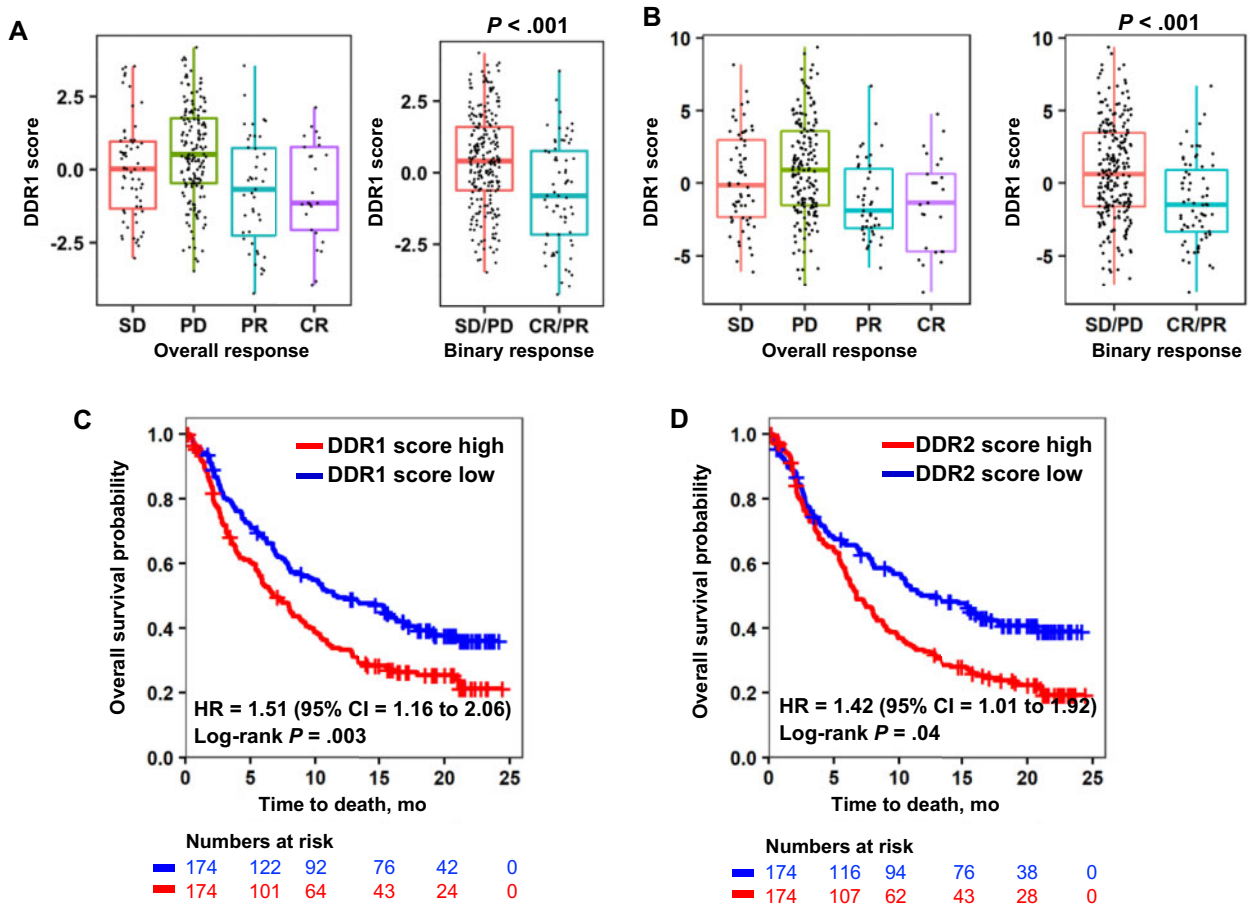


**Figure 5.** Association of DDR gene signature scores with immune checkpoint therapy response of bladder cancer patients. **A, B)** Boxplots depicts DDR1 (**A**) and DDR2 (**B**) scores as a function of the clinical response (stable disease [SD], progressive disease [PD], partial response [PR] and complete response [CR]) from IMvigor. **C, D)** Survival curves for DDR1 (**C**) and DDR2 (**D**) scores in IMvigor. Tumors were stratified into high and low groups at median score levels of IMvigor. Statistical significance of differential survival between the groups was tested by log-rank test. CI = confidence interval; DDR = discoidin domain receptor; HR = hazard ratio.

instability have also been associated with ICT response (42). High TMB has been associated with improved clinical outcome in NSCLC (43), melanoma (44), bladder, and colorectal cancers (42,45-47). The TCGA-BCa and pan-cancer cohorts have shown that DDR2 gene expression has positive association with PD-L1 gene expression, whereas DDR1 gene expression does not (Supplementary Figure 5, available online). Association of DDR gene expression with human leukocyte antigens (HLA) gene mutation could not be confirmed to be statistically significant because of the small number of tumor samples harboring HLA defects in the TCGA data (Supplementary Figure 6 and 7, available online). We also checked the association of DDR gene expression with TMB, resulting in no statistical significance in the TCGA data (Supplementary Figure 8, available online).

The above markers have pan-tumor US Food and Drug Administration approval; however, further improvements are needed in BCa, which motivated the current study. Our work indicates that DDR2 and DDR1 scores have value in stratifying PD-L1 response not only in BCa but also other tumor types, indicating possibly broader utility. These findings reveal intriguing differential biology of DDR1/2 high expression BCa, exhibiting a non-T-cell-inflamed and a T-cell-inflamed phenotype, respectively. Although these are from the same family, our findings revealed their differential involvement regulating immune cell infiltration and a role in the stromal microenvironment in BCa. For instance, in the CheckMate 275

BCa cohort, a high CD8+ T-cell infiltration together with a low EMT and stromal core signature was associated with the highest response and longest progression-free survival and OS following treatment with nivolumab (26). Conversely, patients with a high CD8+ T-cell infiltration but also a high EMT and stromal core signature showed a statistically significantly worse progression-free survival and OS (26), implicating a role of the stromal microenvironment in impeding T-cell function and driving ICT resistance (48,49). Future studies will be important to validate the utility of the DDR scores in predicting ICT response in prospective clinical trials. In these studies, when tumor tissues are evaluated, it is particularly important to do so using single cell technologies. Recently, it has been shown that single cell expression profiling of human bladder cancer provides striking novel information that will likely change how we classify tumor subtypes and other established markers in the future (50). If such gene expression scores are predictive, it would be important to determine if this translates to superior outcomes for patients with high DDR1 and/or DDR2 scores treated with DDR1/2 inhibitors such as sitravatinib (48) and dasatinib (10) in combination with ICT in bladder (NCT03606174) and other cancers (lung: NCT02750514, hematologic NCT02819804, NCT02011945).

In conclusion, these results suggest that DDR gene signatures define differential T-cell tumor-infiltration biology and stratify patient survival following PD-L1 checkpoint inhibitor

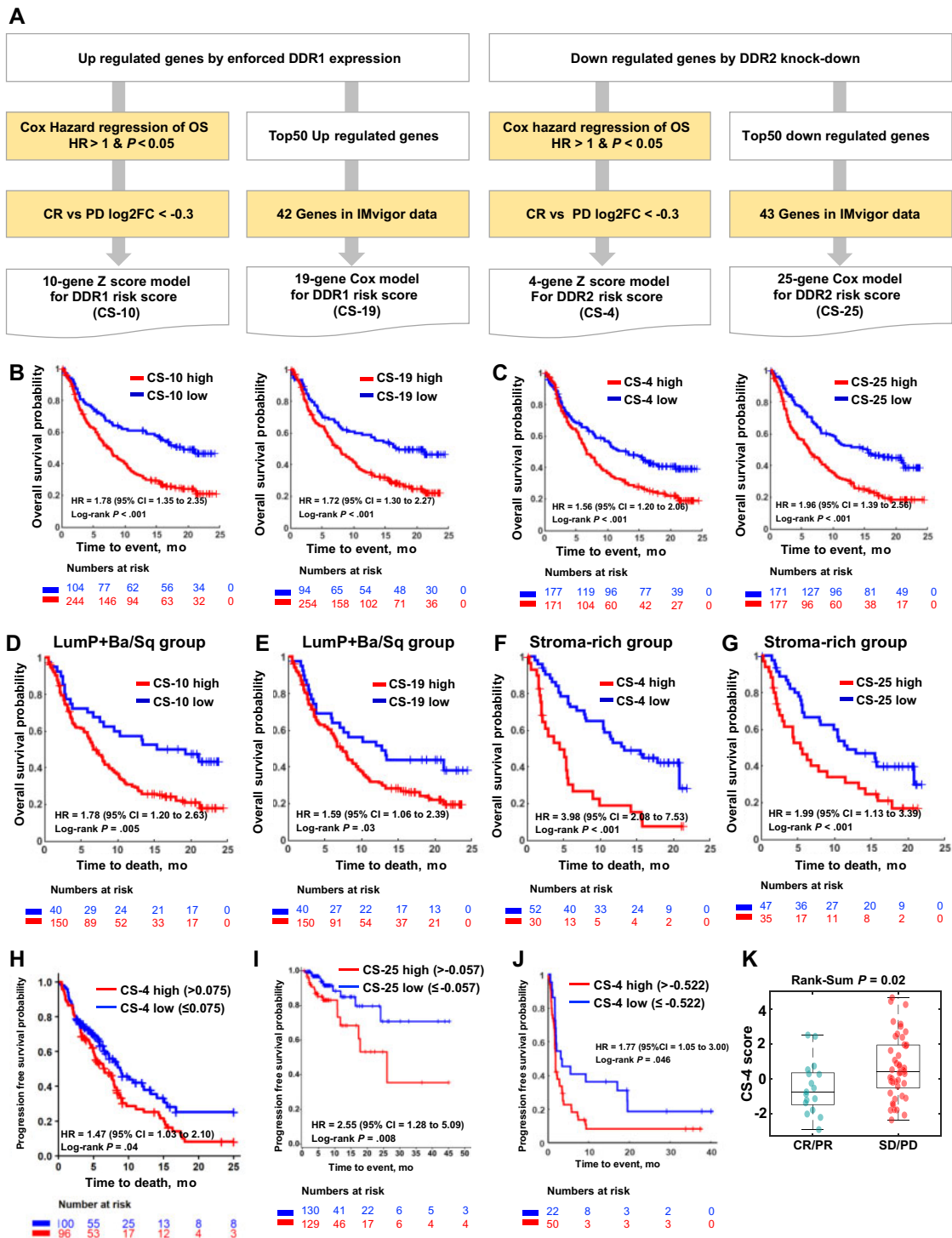


**Figure 6.** Optimization and validation of DDR gene signature scores as predictors of tumor response to anti-PD-L1 therapy. **A)** Schematic diagram of the gene selection process for model construction. Given the upregulated or downregulated genes from DDR murine models, 2 branches of subtractive approaches were employed to make 2 different gene models based on the gene signatures for DDR1 and DDR2, respectively, which correspond to the z score model and Cox model. **B)** Clinical association of DDR1 gene models. **Left and right graphs** show survival analysis results for 10-gene DDR1 z score model (CS-10) and 19-gene DDR1 Cox risk score model (CS-19), respectively. **C)** Clinical association of DDR2 gene models. **Left and right graphs** show survival analysis results for 4-gene DDR2 z score model (CS-4) and 25-gene DDR2 Cox risk score model (CS-25), respectively. **D)** Survival curves of CS-10 high and low groups in LumP and Ba/Sq subtypes in IMvigor. **E)** Survival curves of CS-19 high and low groups in LumP and Ba/Sq subtypes in IMvigor. **F)** Survival curves of CS-4 high and low groups in stroma-rich subtype in IMvigor. **G)** Survival curves of CS-25 high and low groups in stroma-rich subtype in IMvigor. **H)** Survival curves of CS-4 high and low groups in NSCLC cohort treated with anti-PD-L1 therapy from the Tempus cohort. **I)** Survival curves of CS-25 high and low groups in the NSCLC cohort treated with anti-PD-L1 therapy from the Caris cohort. **J)** Survival curves of CS-4 high and low groups in the cohort treated with anti-PD-L1 therapy from the CheckMate 275 cohort. **K)** Boxplots depict CS-4 scores as a function of the clinical response as defined in Figure 5, A, from the CheckMate 275 cohort. Ba/Sq = basal and squamous; CI = confidence interval; CR = complete response; DDR = discoidin domain receptor; HR = hazard ratio; LumP = luminal papillary; NSCLC = non-small cell lung carcinoma; OS = overall survival; PD = partial disease; PD-L1 = programmed cell death ligand 1; PR = partial response; SD = stable disease.

therapy in urothelial cancer. Notably, some signatures also stratified outcome of other cancer types such as melanoma. Further research is needed to understand the importance of tumor type in the utility of these various DDR-based signatures. Overall, our findings suggest that the DDR2- and DDR1-dependent transcriptional program defines differential tumor biology, intriguingly, both linked with immunotherapy response.

## Funding

This work was supported by National Institutes of Health CA075115 (DT) and CA175397 (KSC).

## Notes

**Role of the funder:** The study funders had no role in the design of the study; the collection, analysis, or interpretation of the data; the writing of the manuscript; or the decision to submit the manuscript for publication.

**Disclosures:** DS, JA, DM, PJ are employees of commercial entities (Caris and Tempus) as indicated. All other authors declare no competing interests.

**Authors contributions:** Conceptualization: DT. Methodology: KSC, YCL, and DT. Software and Formal analysis: SY and MK. Validation: SY and MK. Investigation: KSC, SY, YCL, and DT. Resources and Data Curation: KSC, DT, DS, JA, DM, PJ, and MDG. Writing—Original Draft: SY, KSC, XPH, MDG, and DT. Writing—Review & Editing: All authors. Visualization: SY and MK. Supervision: DT. Project Administration: DT. Funding Acquisition: DT. and KSC.

## Data Availability

The RNAseq data generated from the DDR1 (GSE191097) and DDR2 (GSE190698) experiments can be found in Gene Expression Omnibus (GEO).

## References

- Sharma P, Allison JP. Dissecting the mechanisms of immune checkpoint therapy. *Nat Rev Immunol*. 2020;20(2):75-76. doi:10.1038/s41577-020-0275-8.
- Tran L, Xiao JF, Agarwal N, Duex JE, Theodorescu D. Advances in bladder cancer biology and therapy. *Nat Rev Cancer*. 2021;21(2):104-121. doi:10.1038/s41568-020-00313-1.
- Sharma P, Allison JP. The future of immune checkpoint therapy. *Science*. 2015;348(6230):56-61. doi:10.1126/science.aaa8172.
- Havel JJ, Chowell D, Chan TA. The evolving landscape of biomarkers for checkpoint inhibitor immunotherapy. *Nat Rev Cancer*. 2019;19(3):133-150. doi:10.1038/s41568-019-0116-x.
- Schneider AK, Chevalier MF, Derré L. The multifaceted immune regulation of bladder cancer. *Nat Rev Urol*. 2019;16(10):613-630. doi:10.1038/s41585-019-0226-y.
- Rouanne M, Roumiguié M, Houédé N, et al. Development of immunotherapy in bladder cancer: present and future on targeting PD(L)1 and CTLA-4 pathways. *World J Urol*. 2018;36(11):1727-1740. doi:10.1007/s00345-018-2332-5.
- Motzer RJ, Rini BI, McDermott DF, et al. Nivolumab for metastatic renal cell carcinoma: results of a randomized phase II trial. *J Clin Oncol*. 2015;33(13):1430-1437. doi:10.1200/JCO.2014.59.0703.
- Robert C, Long GV, Brady B, et al. Nivolumab in previously untreated melanoma without BRAF mutation. *N Engl J Med*. 2015;372(4):320-330. doi:10.1056/NEJMoa1412082.
- Davis AA, Patel VG. The role of PD-L1 expression as a predictive biomarker: an analysis of all US Food and Drug Administration (FDA) approvals of immune checkpoint inhibitors. *J Immunother Cancer*. 2019;7(1):278. doi:10.1186/s40425-019-0768-9.
- Tu MM, Lee FYF, Jones RT, et al. Targeting DDR2 enhances tumor response to anti-PD-1 immunotherapy. *Sci Adv*. 2019;5(2):eaav2437. doi:10.1126/sciadv.aav2437.
- Lee YC, Kurtova AV, Xiao J, et al. Collagen-rich airway smooth muscle cells are a metastatic niche for tumor colonization in the lung. *Nat Commun*. 2019;10(1):2131. doi:10.1038/s41467-019-09878-4.
- Robertson AG, Kim J, Al-Ahmadie H, et al.; for the TCGA Research Network. Comprehensive molecular characterization of muscle-invasive bladder cancer. *Cell*. 2017;171(3):540-556.e25. doi:10.1016/j.cell.2017.09.007.
- Kamoun A, de Reyniès A, Allory Y, et al.; for the Bladder Cancer Molecular Taxonomy Group. A consensus molecular classification of muscle-invasive bladder cancer. *Eur Urol*. 2020;77(4):420-433. doi:10.1016/j.eururo.2019.09.006.
- Corsa CAS, Brenot A, Grither WR, et al. The action of discoidin domain receptor 2 in basal tumor cells and stromal cancer-associated fibroblasts is critical for breast cancer metastasis. *Cell Rep*. 2016;15(11):2510-2523. doi:10.1016/j.celrep.2016.05.033.
- Iafolla MAJ, Selby H, Warner K, Ohashi PS, Haibe-Kains B, Siu LL. Rational design and identification of immuno-oncology drug combinations. *Eur J Cancer*. 2018;95:38-51. doi:10.1016/j.ejca.2018.02.027.
- Agarwal G, Smith AW, Jones B. Discoidin domain receptors: micro insights into macro assemblies. *Biochim Biophys Acta Mol Cell Res*. 2019;1866(11):118496. doi:10.1016/j.bbamcr.2019.06.010.
- Lafitte M, Sirvent A, Roche S. Collagen kinase receptors as potential therapeutic targets in metastatic colon cancer. *Front Oncol*. 2020;10:125. doi:10.3389/fonc.2020.00125.
- Auguste P, Leitinger B, Liard C, et al. Meeting report - first discoidin domain receptors meeting. *J Cell Sci*. 2020;133(4):jcs243824. doi:10.1242/jcs.243824.
- Mariathasan S, Turley SJ, Nickles D, et al. TGF $\beta$  attenuates tumour response to PD-L1 blockade by contributing to exclusion of T cells. *Nature*. 2018;554(7693):544-548. doi:10.1038/nature25501.
- Smith SC, Baras AS, Owens CR, Dancik G, Theodorescu D. Transcriptional signatures of Ral GTPase are associated with aggressive clinicopathologic characteristics in human cancer. *Cancer Res*. 2012;72(14):3480-3491. doi:10.1158/0008-5472.CAN-11-3966.
- Tu MM, Abdel-Hafiz HA, Jones RT, et al. Inhibition of the CCL2 receptor, CCR2, enhances tumor response to immune checkpoint therapy. *Commun Biol*. 2020;3(1):720. doi:10.1038/s42003-020-01441-y.
- Huang DW, Sherman BT, Lempicki RA. Systematic and integrative analysis of large gene lists using DAVID bioinformatics resources. *Nat Protoc*. 2009;4(1):44-57. doi:10.1038/nprot.2008.211.
- Vandenbon A, Diez D. A clustering-independent method for finding differentially expressed genes in single-cell transcriptome data. *Nat Commun*. 2020;11(1):4318. doi:10.1038/s41467-020-17900-3.
- Hou D, Koyutürk M. Comprehensive evaluation of composite gene features in cancer outcome prediction. *Cancer Inform*. 2014;13(suppl 3):93-104. doi:10.4137/CIN.S14028.
- Levine DM, Haynor DR, Castle JC, et al. Pathway and gene-set activation measurement from mRNA expression data: the tissue distribution of human pathways. *Genome Biol*. 2006;7(10):R93. doi:10.1186/gb-2006-7-10-r93.
- Wang L, Saci A, Szabo PM, et al. EMT- and stroma-related gene expression and resistance to PD-1 blockade in urothelial cancer. *Nat Commun*. 2018;9(1):3503. doi:10.1038/s41467-018-05992-x.
- Topalian SL, Hodi FS, Brahmer JR, et al. Safety, activity, and immune correlates of anti-PD-1 antibody in cancer. *N Engl J Med*. 2012;366(26):2443-2454. doi:10.1056/NEJMoa1200690.
- Weber JS, D'Angelo SP, Minor D, et al. Nivolumab versus chemotherapy in patients with advanced melanoma who progressed after anti-CTLA-4 treatment (CheckMate 037): a randomised, controlled, open-label, phase 3 trial. *Lancet Oncol*. 2015;16(4):375-384. doi:10.1016/S1470-2045(15)70076-8.
- Taube JM, Klein A, Brahmer JR, et al. Association of PD-1, PD-1 ligands, and other features of the tumor immune microenvironment with response to anti-PD-1 therapy. *Clin Cancer Res*. 2014;20(19):5064-5074. doi:10.1158/1078-0432.CCR-13-3271.
- Daud AI, Wolchok JD, Robert C, et al. Programmed death-ligand 1 expression and response to the anti-programmed death 1 antibody pembrolizumab in melanoma. *J Clin Oncol*. 2016;34(34):4102-4109. doi:10.1200/JCO.2016.67.2477.
- Faraj SF, Munari E, Guner G, et al. Assessment of tumoral PD-L1 expression and intratumoral CD8+ T cells in urothelial carcinoma. *Urology*. 2015;85(3):703.e1-703.e6. doi:10.1016/j.urology.2014.10.020.
- Powles T, Eder JP, Fine GD, et al. MPDL3280A (anti-PD-L1) treatment leads to clinical activity in metastatic bladder cancer. *Nature*. 2014;515(7528):558-562. doi:10.1038/nature13904.
- Llosa NJ, Cruise M, Tam A, et al. The vigorous immune microenvironment of microsatellite instable colon cancer is balanced by multiple counter-inhibitory checkpoints. *Cancer Discov*. 2015;5(1):43-51. doi:10.1158/2159-8290.CD-14-0863.
- Patel SP, Kurzrock R. PD-L1 expression as a predictive biomarker in cancer immunotherapy. *Mol Cancer Ther*. 2015;14(4):847-856. doi:10.1158/1535-7163.MCT-14-0983.
- Brahmer J, Reckamp KL, Baas P, et al. Nivolumab versus docetaxel in advanced squamous-cell non-small-cell lung cancer. *N Engl J Med*. 2015;373(2):123-135. doi:10.1056/NEJMoa1504627.
- Motzer RJ, Escudier B, McDermott DF, et al. Nivolumab versus everolimus in advanced renal-cell carcinoma. *N Engl J Med*. 2015;373(19):1803-1813. doi:10.1056/NEJMoa1510665.

37. Ayers M, Lunceford J, Nebozhyn M, et al. IFN- $\gamma$ -related mRNA profile predicts clinical response to PD-1 blockade. *J Clin Invest*. 2017;127(8):2930-2940. doi:10.1172/JCI91190.
38. Grasso CS, Tsoi J, Onyshchenko M, et al. Conserved interferon- $\gamma$  signaling drives clinical response to immune checkpoint blockade therapy in melanoma. *Cancer Cell*. 2020;38(4):500-515.e3. doi:10.1016/j.ccell.2020.08.005
39. Fridman WH, Pagès F, Sautès-Fridman C, Galon J. The immune contexture in human tumours: impact on clinical outcome. *Nat Rev Cancer*. 2012;12(4):298-306. doi:10.1038/nrc3245.
40. Tumeh PC, Harview CL, Yearley JH, et al. PD-1 blockade induces responses by inhibiting adaptive immune resistance. *Nature*. 2014;515(7528):568-571. doi:10.1038/nature13954.
41. Taube JM, Anders RA, Young GD, et al. Colocalization of inflammatory response with B7-H1 expression in human melanocytic lesions supports an adaptive resistance mechanism of immune escape. *Sci Transl Med*. 2012;4(127):127ra37. doi:10.1126/scitranslmed.3003689.
42. Samstein RM, Lee CH, Shoushtari AN, et al. Tumor mutational load predicts survival after immunotherapy across multiple cancer types. *Nat Genet*. 2019;51(2):202-206. doi:10.1038/s41588-018-0312-8
43. Rizvi NA, Hellmann MD, Snyder A, et al. Mutational landscape determines sensitivity to PD-1 blockade in non-small cell lung cancer. *Science*. 2015;348(6230):124-128. doi:10.1126/science.aaa1348
44. Roh W, Chen PL, Reuben A, et al. Integrated molecular analysis of tumor biopsies on sequential CTLA-4 and PD-1 blockade reveals markers of response and resistance. *Sci Transl Med*. 2017;9(379):eaah3560. doi:10.1126/scitranslmed.aah3560.
45. Rosenberg JE, Hoffman-Censits J, Powles T, et al. Atezolizumab in patients with locally advanced and metastatic urothelial carcinoma who have progressed following treatment with platinum-based chemotherapy: a single-arm, multicentre, phase 2 trial. *Lancet*. 2016;387(10031):1909-1920. doi:10.1016/S0140-6736(16)00561-4.
46. Powles T, Durán I, van der Heijden MS, et al. Atezolizumab versus chemotherapy in patients with platinum-treated locally advanced or metastatic urothelial carcinoma (IMvigor211): a multicentre, open-label, phase 3 randomised controlled trial. *Lancet*. 2018;391(10122):748-757. doi:10.1016/S0140-6736(17)33297-X.
47. Patel VG, Oh WK, Galsky MD. Treatment of muscle-invasive and advanced bladder cancer in 2020. *CA Cancer J Clin*. 2020;70(5):404-423. doi:10.3322/caac.21631.
48. Du W, Huang H, Sorrelle N, Brekken RA. Sitravatinib potentiates immune checkpoint blockade in refractory cancer models. *JCI Insight*. 2018;3(21):e124184. doi:10.1172/jci.insight.124184
49. Lee YC, Lam HM, Rosser C, Theodorescu D, Parks WC, Chan KS. The dynamic roles of the bladder tumour microenvironment [published online ahead of print June 28, 2022]. *Nat Rev Urol*. 2022. doi:10.1038/s41585-022-00608-y. <https://www.nature.com/articles/s41585-022-00608-y>
50. Gouin KH, Ing N, Plummer JT, et al. An N-Cadherin 2 expressing epithelial cell subpopulation predicts response to surgery, chemotherapy and immunotherapy in bladder cancer. *Nat Commun*. 2021;12(1):4906. doi:10.1038/s41467-021-25103-7.